

Effective Diffusivities in Zeolites

1. Aromatics in ZSM-5 Crystals

SIGFRIDO F. GARCIA AND PAUL B. WEISZ

Department of Chemical Engineering, University of Pennsylvania, Philadelphia, Pennsylvania, 19104

Received April 20, 1989; revised August 31, 1989

Real or apparent inconsistencies of up to several orders of magnitude exist in reported diffusivities of zeolites. Some are caused by differences in definition, usage, and methodologies in their determination. Some result from operating conditions involving transport mechanisms deviating from a strictly stochastic process. Diffusivities effective in non-steady-state methods of determination (e.g., uptake diffusivities) can be translated into diffusivities applicable to characterization of catalytic (i.e., to steady-state) behavior. For *ortho*-xylene and other aromatic molecules in ZSM-5, the magnitude of these diffusivities follows the expectations of shape selectivity; i.e., they decrease systematically with increasing effective minimum dimension of the molecules. These diffusivities are found to be invariant in both temperature and for a 360-fold variation in applied concentration. A mechanistic model for activated zeolite diffusion, involving inernalized molecules of more than one type (energy level), is suggested to be useful in future considerations of the relationship of intrinsic and effective diffusivities and their activation energies to shape, structure, and molecular mechanism. © 1990 Academic Press, Inc.

INTRODUCTION

The Problem

For the classical porous solids, the meaning, methods of appraisal, and use of “diffusivity” are generally familiar. Diffusivities can often be estimated from dimensional and geometric properties of the pore system and the gas pressure. They determine the “jump distance” in the stochastic random-walk process which is characterized by the intrinsic diffusivity for ordinary or Knudsen diffusion (D). In zeolites, where intracrystalline space approaches molecular dimensions, mass transport enters the new regime of “configurational diffusion” (2). Our current knowledge concerning the relationship of effective zeolite diffusivities to the elementary stochastic process, and to the spacial structures of host or guest, is very limited. Moreover, there appear to be large inconsistencies between reported zeolite diffusivities, often by several orders of magnitude. At least in some cases, this suggests nonuniformities

in the definition, interpretation, or translation of “diffusivity” values derived from or applied to different methods or experiments.

This investigation reexamines the relationships between “diffusivities” derived from different methods and mechanistic assumptions, and examines their likely applicability to diffusion behavior (magnitude, concentration, and temperature dependence) in zeolites. What aspects are caused by thermodynamic parameters, as contrasted to the classical stochastic transport parameters (intrinsic diffusivity)? How is structure (shape selectivity) related to each of these? What elementary process is “activated” as reflected by an appreciable temperature dependence?

Since many conditions, including the choice of the zeolite structure, may be involved in determining or complicating the real or apparent transport mechanism, we have chosen a carefully restricted operating space for analysis and experimental determinations:

We use shape-selective diffusion behavior of aromatic molecules in siliceous ZSM-5, because it provides us with a favorably simple model for both analysis and experiment: A well defined multidimensionally intersecting structure ("maze"); a minimum complexity of chemical adsorption sites (no aluminum); long time constants for the overall diffusion/sorption process, which eliminates concerns of thermal gradients and ensures equilibration of molecular states within a local volume element; and we chose conditions to ensure operation involving transport by the least complicated stochastic processes.

The results should provide further orientation in the interpretation of different "diffusivities" and their relevant uses, e.g., those measured in uptake experiments and those used for catalytic investigations; they suggest mechanistic concepts concerning the relationship of molecular structure parameters to shape-selective intracrystalline diffusion behavior; they provide a degree of unification in what have been diverse phenomena in zeolite diffusion behavior.

Background

A complete bibliography of the literature on zeolite diffusivities with appropriate comments could easily fill a monograph. We cite some of the literature which is exemplary (3-49). Most of the studies employ sorption rate (usually uptake) experiments (3-28); others use chromatographic behavior of zeolites in the stationary phase (29-32) and NMR techniques (33-45). Few authors have deduced diffusivity from catalytic behavior (48, 49).

Reported "diffusivities" span a wide range of orders of magnitude for many sorbates and various zeolites, with apparent inconsistencies of several orders of magnitude. The following are some examples: (i) Figure 1 represents an illustration of diffusivities reported by various sources just for benzene on ZSM-5 crystals based on sorptive methods (uptake, desorption, and chromatographic behavior). (ii) "Mem-

brane" observations on mounted large crystals of ZSM-5 led to reported diffusivities for *n*-butane of near 10^{-7} cm²/sec at 20 to 60°C (47), while much smaller magnitudes (10^{-11} cm²/sec) were reported at higher temperatures (120-180°C) elsewhere (32) and also for xylene (18). (iii) Diffusivities for *n*-hexane derived from catalytic behavior (48) appeared to give values larger by some four orders of magnitude than those found from uptake data (18) (extrapolated to the same temperature). A consistent result for the two methods was obtained (49) when, after temperature extrapolations of sorption rate and equilibrium data, Henry's law constant (measured at low temperature) was included in the Thiele modulus. (iv) Many determinations of diffusivities derived by NMR methodologies, for various molecules and zeolites, have resulted in values two to four orders of magnitude larger than sorption-derived diffusivities [see Kaerger and Pfeifer (45), with over a hundred references]. Various phenomena, such as boundary barriers, have been invoked (38), but the issue remains a topic of debate.

A diversity of behavior is observed for diffusivities upon changing concentration. Often, diffusivities are reported to increase with rising concentration. Sometimes, conceptual formalisms of irreversible thermodynamics (Darken's equation) correct the curvatures observed (50), but do not appreciably alter magnitudes. Concentration dependencies often vary for different methods (37, 43).

Riekert (5) and Ruthven (33), among others, have pointed out that many conditions and phenomena may modify not merely magnitudes but the mechanistic principles involved in the overall diffusion behavior.

In summary, the many investigations have yet to yield a unifying picture for the phenomena, mechanisms, magnitudes, and meaning of "diffusivities" that are effective in describing zeolite behavior, and particularly as they should apply to catalysis in

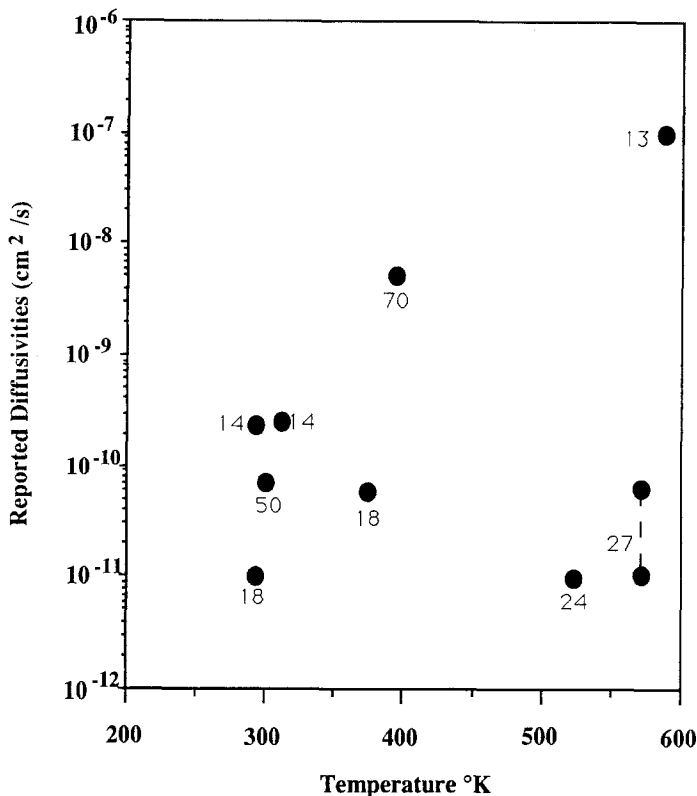


FIG. 1. Reported diffusivity of benzene in the ZSM-5 zeolite structure. Numbers identify source by reference.

zeolites, their unique activities and shape selectivities.

ANALYSIS AND INTERPRETATION OF DIFFUSIVITIES

The interpretation of measurements in terms of "diffusivities" depends importantly on the definitions and mode of usage of the formalisms (usually the Fick equations). They, in turn, depend on mechanisms implied or assumed. As a result, in the science and technology of catalysis and sorption rate phenomena, there exist such diverse terms as "effective," "apparent," "intrinsic," "uptake," "steady-state," and "non-steady-state" diffusivities. Haynes (51) has recently reviewed this topic in relation to the porous solids generally, and pointed to the past confusion that has resulted from this multiplicity of treatment and meaning. In his brief dis-

cussion of zeolites, he introduces another and distinct "zeolitic diffusivity." We extend and broaden the analysis for relating such "diffusivities" to alternative mechanistic models of diffusion in zeolites and specifically to the role of the intrinsic stochastic process of diffusion related to the molecular shape selectivity.

Characterization and Definition of Diffusivities

Fick's first law expresses the statistical fact of a proportionality of the net displacement rate (net flux) to the difference between the existent population densities (concentrations) of mobile species across a volume element with a proportionality constant D :

$$\text{flow rate} = -Ddc/dx. \quad (1)$$

This diffusion constant, or intrinsic diffu-

sivity, is related to mobility parameters of the stepwise statistical events, such as an average jump distance l and an average kinetic velocity v . For a three-dimensional medium

$$D = \left(\frac{1}{3}\right)plv, \quad (2)$$

with p the probability of a successful propagative jump (usually assumed to be $1/2$). D characterizes the structure of the "maze." If, in a zeolite, obstruction of channels occurs, p and therefore D will decrease (and may vary in space and time) because the structure of the "maze" itself is altered. We confine our analysis and experimental observations to conditions where such a change can be neglected.

Fick's second equation expresses a mass balance for each volume element by equating the difference between the in- and outflux of molecules as given by (1) to the resulting accumulation (or depletion) of molecules:

$$D\partial^2c/\partial x^2 = \partial c/\partial t. \quad (3)$$

Having evolved in relation to classical gases and molecular assemblies, it contains the inherent assumption that all molecules contribute equally to the process of stochastic displacement: Use of the same concentration parameter c on both sides of (3), implies that the molecules that at any one time participate in the statistical process driven by the gradient of the mobile species [in (1) or left side of (3)] are identical to those total molecules which represent the accumulation or depletion on the right side of (3). If, at any one time, molecules in a mobile state exist internally only with a concentration c_m , while the total concentration is c_T (i.e., including both mobile and immobilized species), we must, in place of (1) and (3), write

$$\text{flow rate} = -Ddc_m/dx \quad (4a)$$

$$D\partial^2c_m/\partial x^2 = \partial c_T/\partial t, \quad (4b)$$

and a solution of (4b) is possible only if the functional interdependence between the

concentration species c_m and c_T is known. If local mobilization and immobilization are subject to kinetic transitions, no simple solution will be meaningful. On the other hand, equilibrium considerations between energy states can provide such information if, in a sufficiently small macroelement of volume, a local equilibrium between these two species is approached in a time interval short compared to that of the overall process to be evaluated (such as the uptake measurement). Such an equilibrium relationship will be given by an isotherm, i.e., by thermodynamic properties of the system.

For the case of linear isotherm relationships, we have at the inner particle boundary

$$c_T = c_{T\infty} = hc_0, \quad c_m = c_{m\infty} = mc_0, \quad (5)$$

where h is Henry's law constant in the (externally measured) sorption isotherm, and m is the equilibrium ratio of the concentration of the species in the mobile state within the zeolite to that external to the boundary, c_0 .

With (5) and $f = f(x)$ being the fractional depletion of concentration from the boundary ($f = 1$ at $x = 0$), Eq. (4b) becomes

$$D\{m/h\} \partial^2f/\partial x^2 = \partial f/\partial t. \quad (6)$$

Diffusivity determinations based on evaluation of a non-steady-state process (uptake rate or chromatographic behavior) require use of formula (6). The routine application of Fick's equation (1) will therefore generate an effective ("non-steady-state") diffusivity D_{ns} which differs from the intrinsic stochastic diffusivity D by

$$D_{ns} = (m/h) D \quad \text{or} \quad D_{ns} = (mc_0/c_{T\infty})D, \quad (7)$$

where $c_{T\infty}$ is the total equilibrium amount sorbed at the applied concentration c_0 . The diffusivity D_{ns} thus reflects thermodynamic properties in addition to characteristics of the stochastic process.

In the Appendix, we show that regardless of isotherm curvature, the relationship be-

tween the intrinsic stochastic diffusivity and the effective diffusivity derived from a non-steady-state measurement and traditional Fick evaluation will be

$$D_{ns} = \beta(m c_0 / c_{T\infty}) D, \quad \beta = 1.0 \text{ to } 0.6. \quad (8)$$

Exact values of β depend on the curvature of the isotherm (see Appendix), but such correction is seen to be of minor importance compared to the potentially very large factor correction ($m c_0 / c_{T\infty}$).

For the steady-state catalytic process, and since k is customarily defined (and generally only known) in reference to the external concentration c_0 , we have

$$D \partial^2 c_m / \partial x^2 = k f c_0.$$

Since $c_m = m f c_0$

$$(mD) \partial^2 f / \partial x^2 = k f.$$

In relation to the intrinsic diffusivity D , the effective diffusivity D_{ss} in the steady-state process of catalysis is seen to be

$$D_{ss} = mD. \quad (9)$$

Thus, we note the existence of two kinds of diffusivity values that can result from different methods of experiment and analysis, and the relationship of these to the intrinsic diffusivity D intended to describe the traditional stochastic process per se.

Mechanistic Models: Porous Solids and Zeolites

Past usage, as discussed in more detail by Haynes (51), and the extensions to our considerations of zeolite diffusivities are related as follows:

Case 1. In the classical porous medium, we have a mobile medium (gas) which is continuous in concentration across the boundary, $m = 1$, and no immobilization by adsorption, $h = 1$. Thus the classical and unmodified Fick equations are applicable, and any diffusivities derived represent the intrinsic diffusion coefficient D .

Case 2. In classical porous media, but with a capacity of immobilization by adsorption on the pore walls, we still have a continuous concentration of the mobile species across the boundary, $m = 1$, but now $h > 1$.

These two cases are thoroughly reviewed by Haynes in "The Experimental Evaluation of Catalyst Effective Diffusivity" (51). The nonequivalence of various effective diffusivities has also been encountered and described in other systems, such as in the uptake of dye molecules by natural and synthetic fibers (52, 53). As noted there (51), diffusion in zeolites has in most cases been interpreted in terms of a "single phase sorption" model:

Case 3. In that case, the assumption is made that all of the molecules internally sorbed are equally mobile, i.e., $m = h$. We see then from (7) and (9) that the effective diffusivity in an uptake (or other nonequilibrium method of derivation) is the intrinsic stochastic diffusivity, and the effective steady-state diffusivity is h times greater:

$$D_{ns} = D, \quad D_{ss} = hD = (c_{Tz} / c_0 \beta) D. \quad (10)$$

The assumption that at any one moment all internalized molecules participate equally in stochastic motion need not apply to all zeolites or circumstances. Molecules in various positions with respect to the framework atoms (or atomic components such as Al) have been shown to exist in a multiplicity of energy states, by calorimetric studies (54–56) and by computation of adsorptive energy states (57–63). Thus, at any one time, only a fraction of molecules may constitute the population participating in the stochastic transition. We therefore retain the more general model, which becomes

Case 4. The internal population is greater than the applied external concentration, so that $h \gg 1$; but only a fraction of the latter is mobile at any one time, constituting a mobile concentration that need not be equal to the external mobile concentration, i.e., $m <, =, > 1$; as in (7), (8), and (9). This general case is

$$D_{ns} = (m/h) D = \beta(m c_0 / c_{T\infty}) D, \quad D_{ss} = mD. \quad (11)$$

We will be considering this general case for the examination of zeolite behavior. It is analogous to that of a classical porous substance, filled with a liquid, with gas-phase molecules applied externally (c_0), the solubility of which is such that the mobile species in the liquid has a different (higher or

lower) concentration, so that $c_{m\infty}/c_0 = m$, and adsorption sites create an isotherm characterized by h or $c_{T\infty}/c_0$. In fact, mechanistically, the mobile molecules in the zeolite correspond to those in the liquid, except that they are under the influence of the surrounding interactive fields of the crystal structure rather than of the surrounding liquid. An analogous model has been used for polymer membrane systems (64).

APPLICATION

ZSM-5 Zeolite as the Diffusion Medium

To focus on the stochastic diffusion mechanism, we have attempted to make the choice of the zeolite and operating conditions such as to minimize the complexity of parameters that may influence the mass transport phenomenon.

We have chosen ZSM-5 as the zeolite because of its high density of intersections, which are less than two molecular lengths apart, and operating conditions for the measurement of sorption rates confined to low sorptive coverage. This provides minimal self-obstruction of the "maze." We use large enough molecular diffusants, aromatics, to ensure a slow enough overall transport process to allow reasonably adequate approach to equilibrium conditions in a sub-macroscopic volume element (see Analysis): The course of an adsorption measurement involves a time span of a large fraction to several hours. We also confined all studies to sufficiently high temperatures to avoid transition to a mechanism which may be dissimilar to simple stochastic transitions.

In addition, ZSM-5 is a desirable experimental test zeolite because of its availability with almost any degree of Al substitution, from a nearly pure silica structure to one containing a large number of polar substituents (e.g., Al, cations). Also, structural studies have provided information on the relative energy states of aromatic molecules, indicating the existence of a deep adsorptive state at the intersections and shall-

lower positions in the connecting channels needed for the stochastic progression (59, 60). This provides an experimental model for the examination of Case 4; i.e., molecules at channel intersections are the immobilized species strongly attracted to the framework, while molecules between channel intersections are the mobile entities.

Constancy of the Stochastic "Maze"

Obstruction of zeolite intersections in sufficient numbers by temporarily immobilized molecules would lead to a decline of the intrinsic diffusivity by alteration of the "maze" structure [decreasing p in formula (2)]. To avoid such variation we have (i) chosen ZSM-5 as the test zeolite, because its two-dimensional network of 0.7 mmol of intersections per gram of zeolite provides cross-passages at distances less than two molecular dimensions apart; and (ii) use conditions of low coverage, i.e., for calculating uptake rates we use the data for sparse coverage, not exceeding 0.02 mmol of sorbate molecules per gram of zeolite.

An experimental test to ensure minimal effects of self-plugging is carried out by comparing the initial sorption rate of *para*-xylene before and after partial sorption of the bulkier *ortho*-xylene. Figure 2 shows a typical test run. It demonstrates negligible inhibition of the penetration rate by the pre-sorption of *ortho*-xylene.

Temperature Limits for a Stochastic Transport Regime

In simple stochastic thermal motion of molecules, executing random jump events in a pore structure, we deal with individual molecules with no mutual interaction. Such a situation is dependent on certain conditions of temperature and vapor pressure (or population density). Otherwise, concerted molecular behavior phenomena set in, which in the limit of classical pore models result in the onset of "capillary condensation," "capillary flow," or "surface spreading," where the entire ensemble seeks a position of minimal energy of inter-

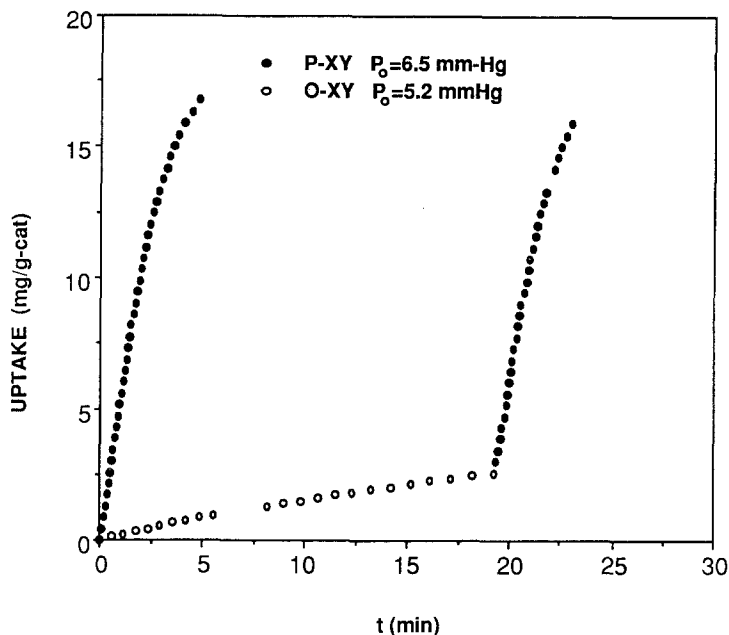


FIG. 2. Test for freedom of "self-plugging" by preadsorbed molecules: Sorption rate of *p*-xylene before and after partial uptake of the bulkier *o*-xylene. Preadsorption of the slow-diffusing *o*-xylene does not significantly alter the rate of subsequent entry of *p*-xylene.

action with their environment. Some aspects of the mass uptake, such as the square root of time dependence, appear similar to diffusion, and can lead to an apparent "diffusion coefficient" (65).

For classical pore radii, the onset conditions for condensation and the velocity of capillary transport are derived from macroscopic parameters of capillary radii, such as surface tension, density, and viscosity (66).

The classical formalisms cannot be expected to quantitatively apply to an approach of the containing structure toward molecular dimensions. However, the basic phenomenon responsible, namely, the extensive influence of the "surface" force fields on the assembly, is still operative. It is of some orienting interest to examine the classically predicted magnitudes of pore radii and operating conditions (p/p_0), at which "capillary condensation" would be expected.

For example, for *o*-xylene at 140°C (density = 0.77 mg/cm³, surface tension = 18.3

dyn/cm), the onset of condensation should occur at

$$\begin{array}{cccc} p/p_0 = & 0.007 & 0.054 & 0.232 & 0.480 \\ \text{for } r(\text{\AA}) = & 2 & 5 & 10 & 20 \end{array}$$

We have probed the conditions for which a transition of mechanism of transport may be indicated by irregularities in the dependence of the initial sorption rate versus temperature. In our study, we observe such indications as we proceed to lower temperatures: For example, as shown in Fig. 3, we find such transitions (*o*-xylene) somewhere below about 140°C at $p \approx 6$ mm Hg, corresponding to $p/p_0 \approx 0.01$. (This magnitude is quite consistent with the values above, considering that the "dimension" of the zeolite "pore" is certainly in the range of $r < 3 \text{ \AA}$).

To limit the analysis to the stochastic molecular transport, the experimental work has then been confined to the temperature and pressure conditions which lie above the mechanistic transitions indicated by measurements as illustrated in Fig. 3.

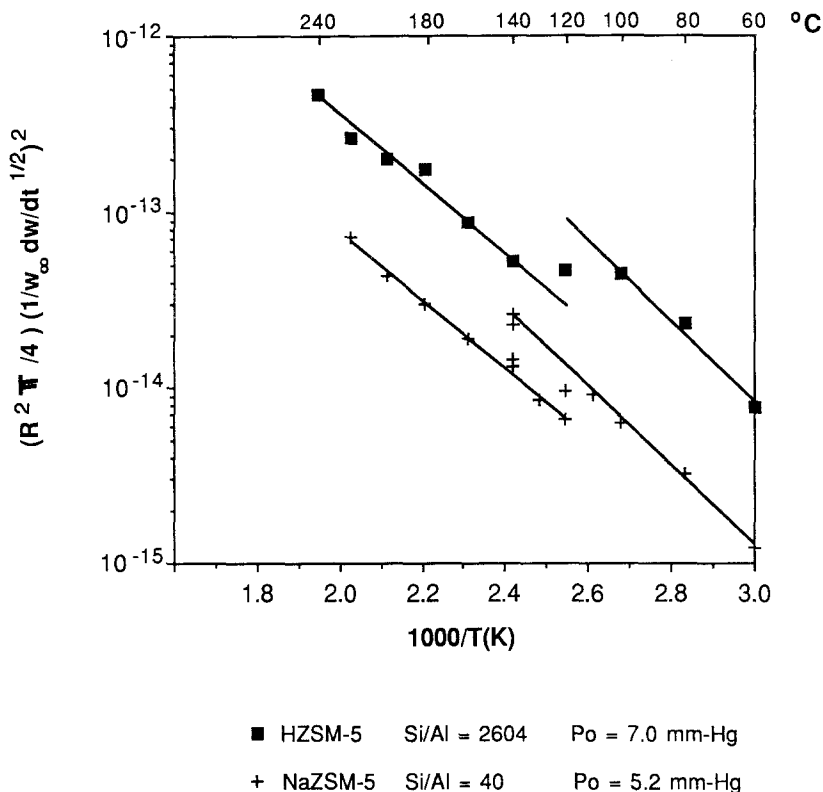


FIG. 3. Evidence of transition of diffusion to a different mechanism of transport at low temperature: Characteristic initial uptake rates as used to derive diffusivities observed for *o*-xylene as a function of temperature. At a sufficiently low temperature a marked and sometimes unstable transition occurs to higher than expected rates.

Experimental Procedures

In this study, apparent non-steady-state diffusivities D_{ns} were derived from gravimetric analysis using a Cahn 1000 microbalance.

For each run, a pure He flow was bubbled through the liquid sorbate at a constant temperature T , fixing the sorbate vapor pressure in the bulk gas phase P by further condensation at a temperature $T_{sat} < T$. To keep P constant, temperatures after the condenser were higher than T_{sat} .

At time zero the zeolite sample in the balance was exposed to the sorbate-He flow, keeping the catalyst temperature T_c constant with a temperature-controlled furnace. Uptake loadings were measured as a function of time, from which uptake rates

($dw/dt^{1/2}$) as well as final loadings (w_∞) were determined. Diffusivities were calculated from conventional solutions [Eq. (13) in the Appendix] of the classical expression of Fick's second law of diffusion. By controlling the furnace and the condenser temperature, diffusion coefficients were obtained at different catalyst temperatures (T_c) and bulk sorbate concentrations ($C_0 = P/RT_c$).

The zeolite samples consisted of ZSM-5 crystals prepared by conventional reported methods (67). Two different Al concentrations were used (Si/Al = 2600 and 40); these Si/Al ratios were determined by quantitative microanalyses. Scanning electron microscopy showed the crystals to have platelike morphology with thickness of 0.5 and 0.7 μm for the low and the high Al zeolite, respectively.

Both protonated and Na-exchanged ZSM-5 samples were obtained from the "as synthesized" zeolite, which contains Na^+ , template ions (i.e., tetrapropylammonium, TPA^+), and some protonic sites. After thermal degradation of the occluded template, $\text{NH}_4\text{-ZSM-5}$ and the final Na-ZSM-5 were obtained by ion exchange at room temperature in solutions of 1 *N* NH_4Cl and 1 *N* NaCl , respectively. The final H-ZSM-5 was obtained after heating the $\text{NH}_4\text{-ZSM-5}$ in dry air at 540°C for 4 h.

Between experiments, samples were regenerated by calcining in a He flow at 540°C , cooling to 300°C , and finally burning at 540°C in air. The temperatures were increased at rates of $2^\circ\text{C}/\text{min}$ to avoid any change in the zeolite framework.

Gas samples of the sorbate-He flow before and after the catalyst were analyzed in a gas chromatograph to ensure the absence of catalytic activity as well as the purity of the sorbate investigated.

Concentration Dependence of Diffusivities

Measurements of uptake behavior and equilibrium sorption were made for *o*-xy-

lene over a 360-fold range of vapor pressures from 0.1 to 36 mm Hg, and at temperatures from 140 to 240°C . The results for the effective non-steady-state diffusivities D_{ns} , as measured, are reported in Fig. 4. These were obtained by the conventional use of the classical solution to Fick's equation given by the initial slope of the uptake runs. They show the frequently reported rise with applied concentration, c_0 , at all temperatures.

Equilibrium sorption isotherms for the same range of pressure and temperatures are shown in Fig. 5. They provide the values for the accumulation factors $c_{T\infty}/c_0$ summarized in Table 1.

The effective steady-state diffusivities D_{ss} , obtained from (11) with the data in Table 1 and $\beta = 1$, are shown in Fig. 6.

$$D_{\text{ss}} = D_{\text{ns}}(c_{T\infty}/c_0)(1/\beta), \quad \beta = 1.0 \text{ to } 0.6 \quad (12)$$

They are larger than the uptake diffusivities D_{ns} by two to four orders of magnitude. The concentration dependence (increase) is fully and consistently eliminated over a

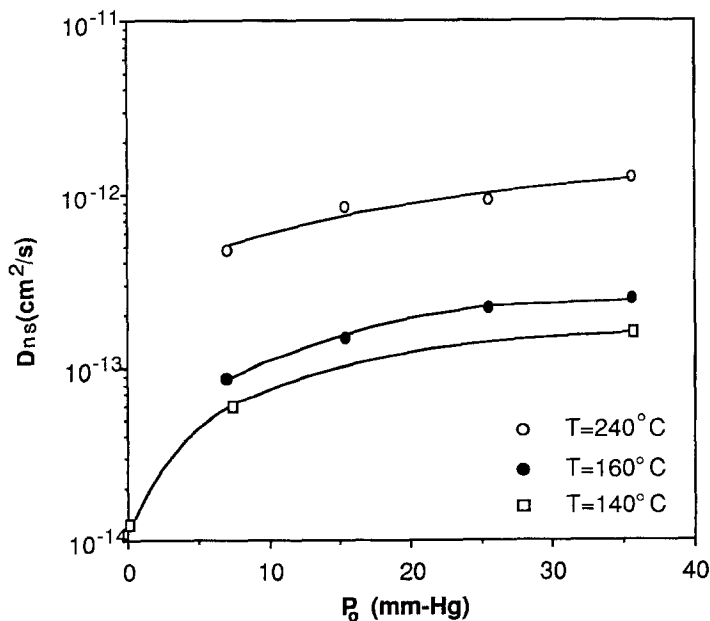


FIG. 4. Concentration dependence of the non-steady-state diffusivities (D_{ns}) of *o*-xylene in siliceous HZDM-5 zeolite (Si/Al = 2604).

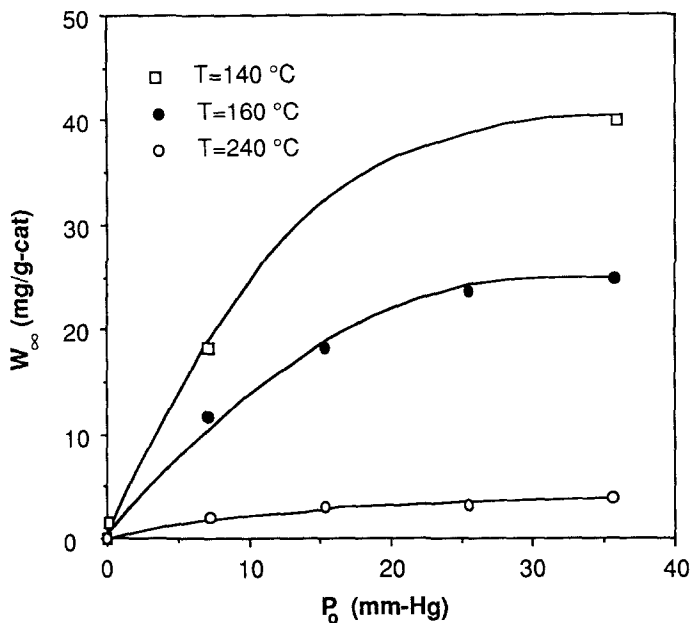


FIG. 5. Sorption isotherms for *o*-xylene in HZSM-5 (Si/Al = 2604).

concentration range spanning a factor of 360, at three different temperatures.

Temperature Dependence and "Activation Energies"

Diffusion coefficients D_{ns} of *o*-xylene were determined over the temperature range 140 to 300°C, at 7.0 and 35.6 mm Hg and over 60 to 140°C for 0.1 mm partial pressure¹ (see Fig. 7). The steady-state diffusion coefficients D_{ss} were determined by measurement of $c_{T\infty}$ and application of (11) as above, and are shown in Fig. 8. Steady-state coefficients were larger than non-steady-state values by two to five orders of magnitude.

The "activation energy" of the uptake diffusivity D_{ns} corresponds to 9 kcal/mol. However, it is seen to arise entirely from the variation of the equilibrium property $c_{T\infty}/c_0$; it influences the overall accumulation time in an uptake situation, but appears

to have no relevance to the transport property of molecules in motion.

On the other hand, the steady-state diffusivity D_{ss} remains invariant with temperature, for the diffusant *o*-xylene and the zeolite ZSM-5 employed. This does not appear to be accidental nor entirely unique: We have added to Figs. 7 and 8 results obtained with *p*-xylene and with 2-methyl naphthalene on another sample of ZSM-5. These combinations, too, exhibit the analogous behavior.²

DISCUSSION AND CONCLUSIONS

Magnitude of Measured Diffusivities

We have shown that important changes in the transport mechanism may occur at low temperatures (for our sorbate/zeolite case, at or above $p/p_0 = 0.01$). They are not likely to be describable by the classical concepts of a stochastic diffusion mechanism.

¹ At 0.1 mm Hg pressure of *o*-xylene, no transition of mechanism was discernible down to 60°C.

² Cross-comparisons among these aromatic diffusants and *o*-xylene are not necessarily meaningful since they involve different ZSM-5 compositions.

TABLE I
Accumulation Factors $c_{T_{\text{res}}}/c_0$ for *o*-Xylene in
Siliceous ZSM-5

Temperature (°C)	P (mm Hg)				
	0.1	7	15	25	36
140	20,846	3540	—	—	1520
160	—	2330	1670	1310	980
240	—	510	340	210	180

This may apply to some of reported diffusivity data collected in Fig. 1. Diffusivity studies of isobutane permeation through an NaX crystal (46) at 25°C and corresponding to p/p_0 values between 0.03 and 0.15 presented symptoms of large instabilities in flow which are characteristic of "capillary flow" or "surface spreading" behavior. The separation of components (isobutane from methane), observed in this study, is also remindful of selective "capillary condensation" of the higher-molecular-weight material.

Even if measurements are made under conditions of comparable mechanism (stochastic behavior, no alteration of the "maze" structure, etc.), "agreement" of diffusivities as reported and determined by various methods may generally not be apparent, because of differences in modes of usage, definition of terms (especially of concentration), and assumed mechanistic models, as noted by Haynes (51) and elaborated for zeolites above.

In catalytic behavior and practice, kinetic parameters and diffusion inhibition criteria are generally referred to the operating concentrations, c_0 (or pressures), of reactants. They deal with diffusion processes in the steady state. The appropriate diffusivities D_{ss} are derived from diffusivities obtained from non-steady-state processes (uptake, desorption, or their combined effect in the chromatographic method), D_{ns} , by formula (12). For that translation, knowledge of the parameter m is not required.

Reported diffusivities based on uptake rate, desorption rates, or chromatographic

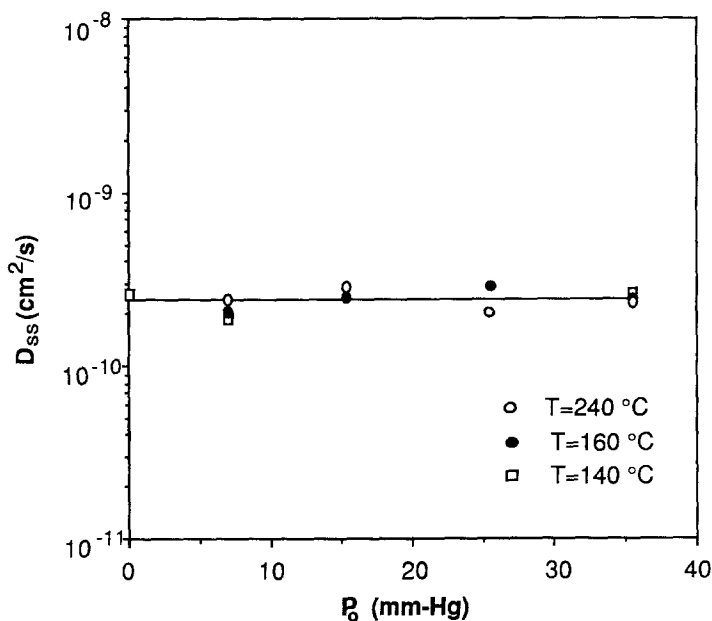


FIG. 6. Concentration dependence of steady-state diffusivities (D_{ss}) of *o*-xylene in HZSM-5 zeolite (Si/Al = 2604).

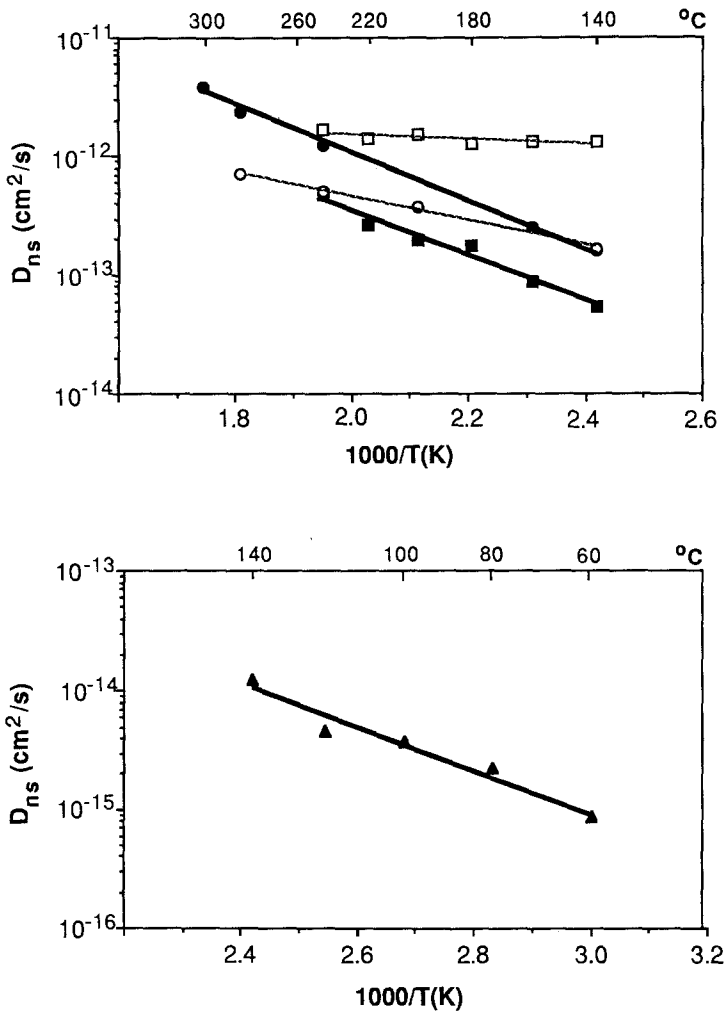


FIG. 7. Temperature dependence of non-steady-state diffusivities (D_{ns}) in ZSM-5 zeolite.

Molecule	Pressure (mm Hg)	ZSM-5 zeolite	
		Cation form	Si/Al ratio
● o -Xylene	35.6	H	2600
■ o -Xylene	7.0	H	2600
▲ o -Xylene	0.1	H	2600
□ p -Xylene	6.5	Na	40
○ 2-Methyl naphthalene	5.4	Na	40

techniques are all based on evaluation of D_{ns} and should provide comparable results among themselves, as reported. To the extent that comparisons exist of similar sorbates, zeolites, and temperature conditions, the literature bears this out [e.g.,

Chiang *et al.* (32), Goddard and Ruthven (44), Eic and Ruthven (68)].

Effective steady-state diffusivities, D_{ss} , should be and are generally two to five orders of magnitude larger. This is consistent with the observed magnitudes of catalytic-

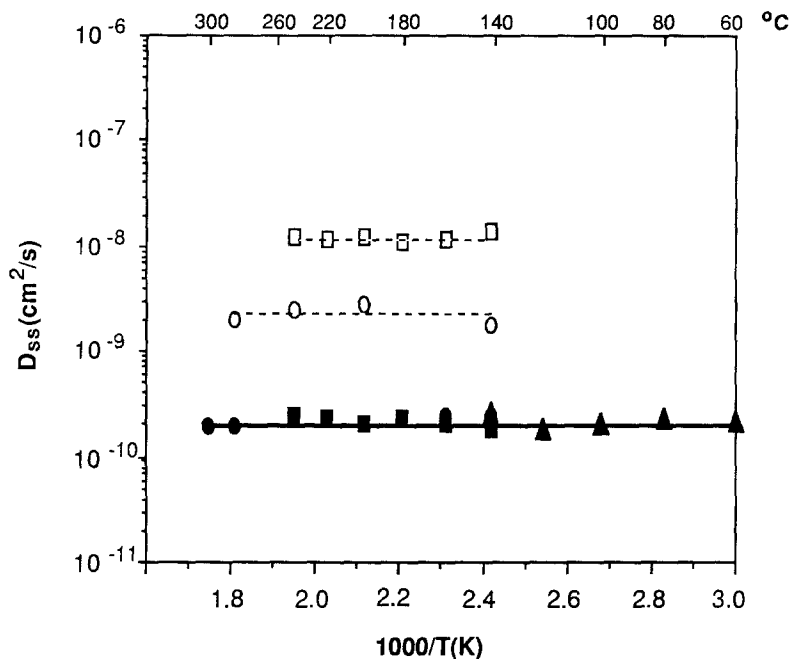


FIG. 8. Temperature dependence of steady-state diffusivities (D_{ss}) in ZSM-5 zeolite. Sample identifications are same as in Fig. 5. All *o*-xylene data (filled-in symbols), including variations of 350:1 in applied pressure, appear on constant line. Dashed lines represent *p*-xylene and 2-methyl naphthalene data.

cally effective diffusivities observed by Haag *et al.* (48). Also, by Post *et al.* (49) obtained comparable magnitudes of catalytic and uptake diffusivities for 2,2-dimethyl butane—albeit involving considerable temperature extrapolations—after including an estimated Henry's law constant h in the modified diffusion criterion based on only observable quantities (1*b*), as

$$F = (dn/dt)(1/c_0)(R^2/hD_{ns}),$$

thus performing the transformation to D_{ss} , as in (12).

For *o*-xylene on ZSM-5, we find the effective steady-state diffusion coefficients D_{ss} to be constant over the concentration range 360 to 1. This is in line with the expectation for a stochastic diffusion process under conditions which do not change the "structure of the maze" or involve a mechanistic transition when appreciable intermolecular interactions sets in.

The importance of D_{ss} for considering

mechanistic aspects in shape-selective catalysis is illustrated by the observation (Figs. 7 and 8) that the order of the D_{ss} magnitudes follows the logical (inverse) order of the smallest molecular dimension of the molecules, which is³ *p*-xylene < 2-methyl naphthalene < *o*-xylene. This logical relationship is not found in the behavior of the diffusivities D_{ns} measured by the non-steady-state methods [without the transformation (12)].

However, neither D_{ss} nor D_{ns} necessarily represent intrinsic stochastic diffusivities (2), as seen from (11) and (12).

Mechanism of Activated (Shape-Selective) Diffusion

Consideration in detail of Cases 3 and 4 is helpful in examining mechanistic aspects of

³ Note that for methyl naphthalenes the smallest cross section is highly dependent on the position of the methyl group. 1-Methyl naphthalene would exceed *o*-xylene in critical dimension.

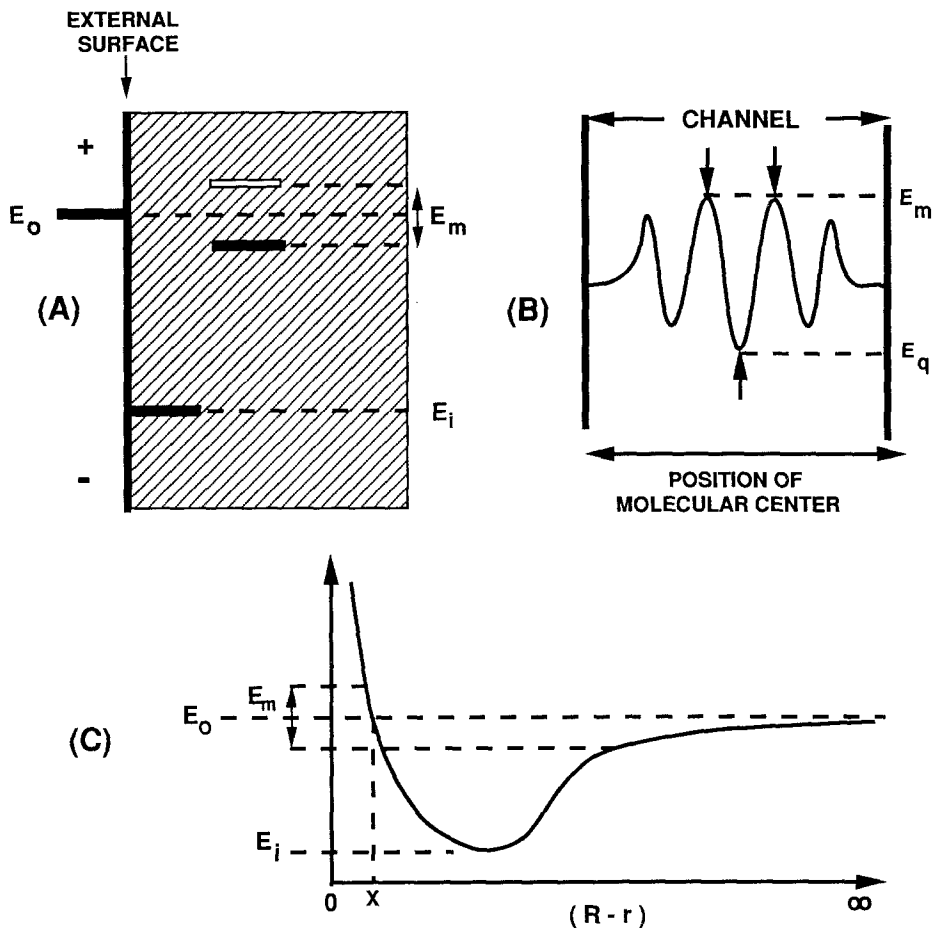


FIG. 9. Energy states in zeolites. (A) E_i = molecule in most stable adsorbed state (e.g., at intersection in ZSM-5); E_m = minimum necessary energy state for stochastic progression; E_o = external molecule. (B) Illustration of potential energy variation vs position of molecular center along a channel. (C) Illustration of a possible range of E_m , including cases of $E_m > E_o$. The latter implies penetration into a sufficiently repulsive field, i.e., $(R - r) < x$, where r and R represent an effective "radius" for the molecule and the local intrazeolite structure, respectively.

the nature of activated (shape-selective) diffusion, the nature of the intrinsic diffusivity D , the origin of the temperature coefficient, the influence of molecular structure, etc.

ZSM-5 zeolite, for instance, offers a structure favorable for examining Case 4. Aromatic molecules have been shown to exist in two types of equilibrium states (59, 60): a deep energy state positioned in a channel intersection, and weaker potential energy states in channel positions between intersections. For *p*-xylene in substantially

aluminum-free ZSM-5, Reischman *et al.* (60) have indicated a -19.6 kcal/mol level for the intersection and -11.5 and -7.2 kcal/mol stable levels for channel positions. Thus, in the network of intersecting channels, and with sparse coverage, molecules will reside at intersections. They will have to pass through a higher-energy-level channel position to execute a progressive random jump.

Figure 9 represents a model representation of the basic elements to be added to the classical diffusion treatment. E_i represents

the most stable (immobilized) level at intersections. E_m is the lowest necessary state that must be attained for entry and passage through a channel. As illustrated in Fig. 9B, this level can be higher than the stablest in-channel level, E_q , which may result from calculation or measurement of equilibrium properties. E_m is analogous to the transition state in reaction rate theory. E_m may lie at, below, or above E_0 . The latter will be the case if the molecule is of such structure and size that its integrated interaction with the zeolite framework atoms results in a net repulsive force in the position of lowest but necessary energy for successful passage; this is illustrated by Fig. 9C, in a manner familiar for a point molecule in relation to the force field experienced upon a progressively closer approach to a "surface."

The population c_T represents the molecules at the deep energy level E_i , at the intersections (the reasonable assumption is made that $c_m \ll c_T$). The diffusivity $D_{ss} = mD$ [see (11)] will exhibit an activation energy only if m , i.e., if the population c_m has an activation energy. This would occur if $E_m > E_0$. In fact, in this investigation, D_{ss} values consistently show negligible activation energies. This need not be anticipated to hold for "tighter fitting" molecules, i.e., when $E_m > E_0$, as noted above. We can anticipate the probability of passing the barrier to depend on E_m , and also on the frequency in which the molecular configuration, as well as spacial position with respect to the "entrance" of a channel, will be favorable. We note that the aromatic molecules in this study are rigid and no configurational variants are possible. This will not be the case for all molecules, as for example in the case of an aliphatic structure or side chain where configurational rotations around one or more bonds will be possible.

If we were to retain the traditional view of Case 3, we would interpret measured diffusivities according to (10). $D_{ns} = D$; i.e., the measured D_{ns} or uptake diffusivities would directly represent the intrinsic (stochastic) diffusivities. The question then

arises of how a stochastic diffusion constant D would exhibit an activation energy. This leads logically to description of a constant stochastic progression term [as in (2)], which, however, involves only a fraction of the population given by the activation energy to pass the barrier E_m , which leads us to the very mechanistic model of activated diffusion already described by our Case 4.

NMR self-diffusivities are said [see (33, 35)] to provide intrinsic (stochastic) diffusivities D as defined by (2). Comparisons with measured D_{ns} or D_{ss} diffusivities, if done under equivalent conditions and at coverages and temperatures ensuring a stochastic transport process, should be able to provide information on the concentration of mobile species $m = c_{m\infty}/c_0$, according to (10) and (11), and further insights into the mechanistic process, Case 3 or 4.

We observe that NMR self-diffusivities, presumed equal to D , have generally been found (40, 43, 44, 68, 69) to be two to four orders of magnitude larger than uptake diffusivities D_{ns} which would be inconsistent with Case 3 for which $D_{ns} = D$ (10). Instead, they appear to be of magnitudes approaching D_{ss} , which suggests applicability of Case 4 and (11). Measurements using NMR techniques will clearly contribute important insights for zeolite diffusion in the future.

The fact that the diffusivities D_{ss} found in this work are invariant over the concentration range 360 to 1 and over a range of temperature, and with similar such behavior for a number of different aromatic molecules, would suggest achievement of a certain valuable degree of unification in the view of "diffusivities" in zeolites. Aside from clarifying matters of meaning, interpretation, and application of variously derived values of zeolite diffusivities, this work suggests the value of considering the existence and mechanistic implications of more than one energy state of molecules participating in the intrazeolite transport process, analogous to the role of the transition state in the treatment of chemical reaction rates.

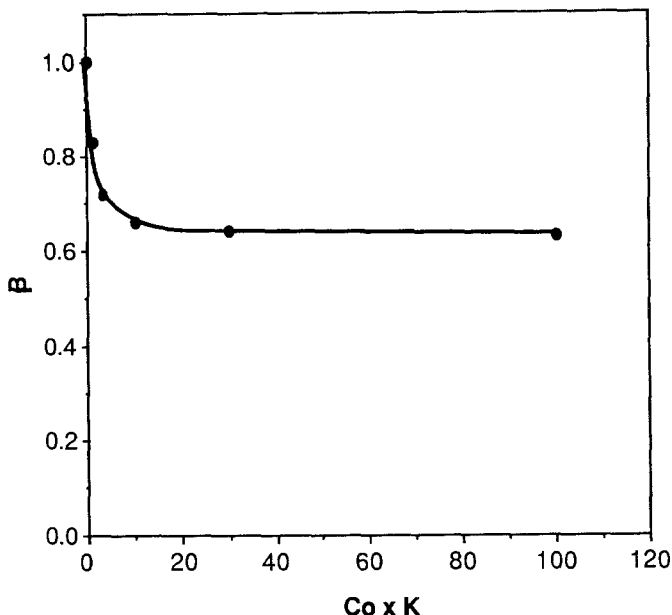


FIG. 10. Correction factor β characterizing the deviation of effective diffusivity derived from an assumption of a linear isotherm, when isotherm is curved (characterized by a Langmuir constant K and applied concentration c_0 , for spherical geometry).

APPENDIX: NONLINEAR ISOTHERMS

Diffusivities are conveniently derived from the observed initial slope of the fractional uptake rate versus the square root of time, according to the classical solution of Fick's second equation,

$$D_{\text{eff}} = (\pi/4)\{(1/w_\infty)(dw/dt^{1/2})^2 L^2$$

(for one-dimensional geometry with thickness L). For linear isotherms we have $D_{\text{eff}} = D_{\text{ns}} = Dm(c_0/c_{T\infty})$, and therefore

$$Dm(c_0/c_{T\infty}) = (\pi/4)\{(1/w_\infty)(dw/dt^{1/2})^2 L^2. \tag{13}$$

For many cases, a Langmuir isotherm, $c_{T\infty} = c_s/c_0/(1/K + c_0)$, with variously strong interaction constants K will be more appropriate to express any reasonably observed isotherm curvature. The error resulting from application of (13) and neglect of the proper functional curvature can be appraised by comparing the (analytically available) solutions of the two limiting cases of the Langmuir isotherm:

When K is small, we have the linear iso-

therm case, and (13) applies. When K is large, we approach, in the limit, irreversible immobilization, where $c_{T\infty} = c_s$ for all $c_0 > 0$. The analytical solution for the resulting "shell-progressive" transport process is available (52, 71, 72). With our nomenclature, it derives from equating the flux per unit area due to the gradient between the surface ($x = 0$) and the position of the "shell" x to the motion of the shell:

$$mc_0D/x = (dx/dt)c_{T\infty} \tag{14}$$

with $dW/W_\infty = dx/L$, and putting the solution into the same format as (13) gives

$$Dm(c_0/c_{T\infty}) = \frac{1}{2}\{(1/w_\infty)(dw/dt^{1/2})^2 L^2. \tag{15}$$

The effective diffusivity thus contains the same correction factor $m(c_0/c_{T\infty})$. Beyond this it differs from that in (13) only by a correction of $\beta = (1/2)/(\pi/4) = 0.64$. Thus, applying the interpretation of diffusivity which assumes a linear isotherm will, for curved isotherms, lead to errors of overestimating diffusivity by at most $1/0.64 = 1.56$.

Values of the correction factor β for conditions between the two limiting cases, i.e., for any curvature characterized by K , can be determined from the numerical solutions of Weisz and Hicks (52), and are plotted in Fig. 10.

ACKNOWLEDGMENTS

The authors acknowledge support, as well as catalyst samples and research equipment, made available by Mobil Research and Development Corporation, Princeton, New Jersey. This research was supported by National Science Foundation Grant CBT-8814120 and in part by the Petroleum Research Fund, administered by the ACS (Grant 20499-ACS).

Note added in proof. One of our reviewers pointed out that the Darken correction, $d \ln c_{Tz}/d \ln c_0$, is proportional to the simple correction factor, c_{Tz}/c_0 , for the mathematical form of the Langmuir isotherm, $c_{Tz} = ac_0/(1/K + c_0)$. This is worthy of wide attention, since this mathematical truth has not been generally appreciated; the procedure of translating (a limited number of) data points into a slope of a double logarithmic plot is, after all, inaccurate and unnecessarily elaborate compared to simply taking the ratio of the measured values of c_{Tz} and c_0 . (We regret that we are unable to credit the reviewer with pointing out this mathematical fact, in view of the practices of covert, i.e., anonymous, reviewing.) Since it is a *proportionality* and not an *equality*, the Darken approach can alter the dependence of diffusivity on concentration, but fails to introduce the *magnitude* corrections discussed in this paper. It is also significant to point out that observed isotherms (including those of zeolites) can be approximated by a Langmuir formalism at any one temperature; but, at different temperatures, zeolite isotherms approach different saturation values, contrary to classical behavior of surfaces.

REFERENCES

1. (a) Wheeler, A., *Adv. Catal.* **3**, 250 (1951). (b) Weisz, P. B., and Prater, C. D., *Adv. Catal.* **6**, 143 (1954).
2. Weisz, P. B., *Chemtech* **3**, 498 (1973).
3. Breck, D. W., "Zeolite Molecular Sieves." Wiley, New York, 1974.
4. Barrer, R. M., *Adv. Chem.* **102**, 1 (1971).
5. Riekert, L., *Adv. Catal.* **21**, 281 (1970).
6. Schirmer, W., *Chem. Technol.* **23**, 23 and 98 (1971).
7. Kiselev, A. V., *Adv. Chem.* **102**, 37 (1971).
8. Riekert, L., *AIChE J.* **17**, 446 (1971).
9. Goring, R. L., *J. Catal.* **31**, 13 (1973).
10. Ma, Y. H., and Ho, S. Y., *AIChE J.* **20**, 279 (1974).
11. Doelle, H. J., and Riekert, L., *ACS Symp. Ser.* **40**, 401 (1977).
12. Buelow, M., et al., *J. Chem. Soc. Faraday Trans.* **76**, 597 (1980).
13. Olson, D. H., Kokotailo, G. T., and Lawton, S. L., *J. Phys. Chem.* **85**, 2238 (1981).
14. Doelle, H.-J., Heering, J., Riekert, L., and Marosi, L., *J. Catal.* **71**, 27 (1981).
15. Heering, J., Kotter, M., and Riekert, L., *Chem. Eng. Sci.* **37**, 581 (1982).
16. Kmiotek, S. J., M.S. thesis, Worcester Polytechnic Institute, 1981.
17. Anderson, J. R., et al., *J. Catal.* **58**, 114 (1970).
18. Wu, P., Debebe, A., and Ma, Y. H., *Zeolites* **3**, 118 (1983).
19. Buelow, M., Kaerger, J., Kocirik, J., and Voloschuk, A. M., *Z. Chem.* **21**, 175 (1981).
20. Kaerger, J., and Ruthven, D. M., *J. Chem. Soc. Faraday Trans. 1* **77**, 1485 (1981).
21. Buelow, M., Lorenz, P., Mietk, W., Struve, P., and Samulevic, N. N., *J. Chem. Soc. Faraday Trans. 1* **79**, 1099 (1983).
22. Buelow, M., Mietk, W., Struve, P., and Lorenz, P., *J. Chem. Soc. Faraday Trans. 1* **79**, 2457 (1983).
23. Le Van Mao, R., Ragini, V., Leofanti, G., and Fois, R., *J. Catal.* **81**, 418 (1983).
24. Pope, C. G., *J. Phys. Chem.* **88**, 6312 (1984).
25. Buelow, M., Struve, P., Mietk, W., and Kocirik, M., *J. Chem. Soc. Faraday Trans.* **80**, 813 (1984).
26. Tezel, D. H., Ruthven, D. M., and Wernick, D. L., in "Proceedings, 6th International Zeolite Conference, 1984."
27. Choudhary, V. R., and Srinivasan, K. R., *J. Catal.* **102**, 312 (1986).
28. Hoelderich, W., and Riekert, L., *Chem. Ing. Tech.* **58**, 412 (1986).
29. Ma, Y. H., and Mancel, C., *AIChE J.* **18**, 1148 (1972).
30. Shaw, D. B., and Ruthven, D. M., *AIChE J.* **23**, 804 (1977).
31. Lechert, H., and Schweitzer, W., in "Proceedings, 6th International Zeolite Conference, 1984," p. 210.
32. Chiang, A. S., Dixon, A. G., and Ma, Y. H., *Chem. Eng. Sci.* **39**, 1461 (1984).
33. Ruthven, D. M., *Sep. Purif. Methods* **5**, 189 (1976).
34. Tanner, J. E., and Stejsal, E. O., *J. Chem. Phys.* **49**, 1768 (1968).
35. Kaerger, J., Pfeifer, H., and Buelow, M., *Z. Chem.* **16**, 85 (1976).
36. Kaerger, J., and Caro, J., *J. Chem. Soc. Faraday Trans. 1* **73**, 1363 (1977).
37. Kaerger, J., and Ruthven, D. M., *J. Chem. Soc. Faraday Trans. 1* **77**, 1485 (1981).
38. Kaerger, J., Heink, W., Pfeifer, H., Rauscher, M., and Hoffman, J., *Zeolites* **2**, 275 (1982).

39. Bulow, M., *Z. Chem.* **25**, 81 (1985).
40. Kaerger, J., and Caro, J., *J. Colloid Interface Sci.* **52**, 623 (1975).
41. Kaerger, J., and Caro, J., *J. Chem. Soc. Faraday Trans. 1* **76**, 1562 (1980).
42. Yasuda, Y., and Yamamoto, A., *J. Catal.* **93**, 176 (1985).
43. Germanus, A., Kaerger, J., Pfeifer, H., Samulevic, N. N., and Zdanov, S. P., *Zeolites* **5**, 91 (1985).
44. Goddard, M., and Ruthven, D. M., in "Proceedings, 7th International Zeolite Conference, 1986;" and *Zeolites* **6**, 283 and 445 (1986).
45. Kaerger, J., and Pfeifer, H., *Zeolites* **7**, 90 (1987) (Review).
46. Wernick, D. L., and Osterhuber, E. J., in "Proceedings, 6th International Zeolite Conference." Butterworth, London, 1983; and *J. Membr. Sci.* **22**, 137 (1985).
47. Paravar, A., and Hayhurst, D. T., in "Proceedings, 6th International Zeolite Conference, 1984," p. 217.
48. Haag, W. O., Lago, R. M., and Weisz, P. B., *Faraday Disc.* **72**, 317 (1982).
49. Post, M. F. M., Van Amstel, J., and Kouwenhoven, H. W., in "Proceedings, 6th International Zeolite Conference, 1984," p. 517.
50. Shah, D. B., Hayhurst, D. T., Evanina, G., and Guo, C. J., *AIChE J.* **34**, 1713 (1988).
51. Haynes, H. W., Jr., *Catal. Rev.-Sci. Eng.* **30**, 563 (1988).
52. Weisz, P. B., and Hicks, J. S., *Trans. Faraday Soc.* **63**, 1801 and 180 (1967).
53. Weisz, P. B., and Zollinger, H., *Trans. Faraday Soc.* **63**, 1967 (1967).
54. Thamm, H., Stach, H., and Fiebig, W., *Zeolites* **3**, 95 (1983).
55. Stach, H., Tamm, H., Jaenche, J., Fiedler, K., and Schirmer, W., in "Proceedings, 6th International Zeolite Conference 1984," p. 225.
56. Thamm, H., *J. Phys. Chem.* **92**, 193 (1988).
57. Williams, D. E., *Acta Crystallogr. A* **25**, 464 (1969).
58. Williams, D. E., *Acta Crystallogr. A* **28**, 629 (1972).
59. Reischman, P. T., and Olson, D. H., in "6th International Zeolite Conference," Poster Session (A Theoretical Study of Hydrocarbon Sorption in ZSM-5) (1983).
60. Reischman, P. T., Schmitt, K. D., and Olson, D. H., *J. Phys. Chem.* **92**, 5165 (1988); also Florida Conference on Catalysis, Palm Coast (1986).
61. Ramdes, S., Thomas, J. M., Betteridge, P. B., Cheetham, A. K., and Davies, E. K., *Angew. Chem. Int. Ed. Engl.* **23**, 671 (1984).
62. Kiselev, A. V., Lopatkin, A. A., and Shulga, A. A., *Zeolites* **5**, 261 (1985).
63. Derouane, E. G., Andre, J., and Lucas, A. A., *Chem. Phys. Lett.* **137**, 336 (1987).
64. Meldon, J. H., Kang, Y.-S., and Sung, N.-H., *I&EC Fundam.* **24**, 61 (1965).
65. Weisz, P. B., *Ber. Bunsenges. Phys. Chem.* **90**, 413 (1975).
66. See, e.g., Bikerman, J. J., "Surface Chemistry," Academic Press, New York, 1948; or Grassmann, P., "Physical Principles of Chemical Engineering," Pergamon Press, Elmsford, NY, 1971.
67. Mobil Oil Corp., The Netherlands Patent 7,014,807 (1971).
68. Eic, M., and Ruthven, D. M., *Zeolites* **8**, 40 (1988).
69. Gelbin, D., *AIChE J.* **25**, 358 (1979).
70. Zikova, A., Bulow, M., and Schlodder, H., *Zeolites* **7**, 115 (1987).
71. See the Tarnishing Reaction in Crank, J., "The Mathematics of Diffusion," pp. 117ff. Oxford Univ. Press, London, 1964.
72. Weisz, P. B., and Goodwin, R. D., *J. Catal.* **2**, 397 (1963).